BULLETIN OF THE EARTHQUAKE
RESEARCH INSTITUTE
UNIVERSITY OF TOKYO
Vol. 64 (1989), pp. 457-485

Three-Dimensional P-Wave Velocity Structure Beneath the Japanese Islands

Shin'ichiro KAMIYA[1], Takashi MIYATAKE[1]
and Kazuro HIRAHARA[2]

[1] Earthquake Research Institute, University of Tokyo
[2] Disaster Prevention Research Institute, Kyoto University

(Received June 30, 1989)

Abstract

A new model of fine three-dimensional *P*-wave velocity structure down to a depth of 1200 km beneath the Japanese Islands and their vicinity is derived by a tomographic inversion of ISC travel time data with resolution analyses. We used 103,023 arrival time data observed at 548 stations from 833 earthquakes to determine the velocity anomalies in a number of blocks and source parameter corrections simultaneously. A block size of $0.5°\times0.5°$ in horizontal dimension and 50 km in depth (for the uppermost three layers $0.5°\times0.5°\times33$ km) was used in this study.

Detailed features of lateral heterogeneity in the upper mantle are revealed. High velocity zones corresponding to the Pacific and Philippine Sea slabs are well delineated. Low velocity anomalies corresponding to the volcanic front are found. High or low velocity anomalies in the crust or uppermost mantle correspond to positive or negative Bouger anomalies. And high velocity anomalies correspond to low heat flow.

In the lower mantle, slab-shaped high velocity anomalies are found extending deeper than the termination of seismic activity within the Pacific slab descending from the Japan Trench. A resolution analysis confirms the existence of the slab-like high velocity region in the lower mantle, though the extent of its depth is not well resolved. On the other hand, the Pacific slab descending from the Izu-Bonin Trench seems to be fingering; that is, high velocity anomalies penetrate into the lower mantle at about 26°N, but do not penetrate and bend horizontally to the west in the deeper portion of the upper mantle at about 29°N.

1. Introduction

Since the works by AKI and LEE (1976) and AKI *et al.* (1977), three-dimensional seismic structures have been investigated in various

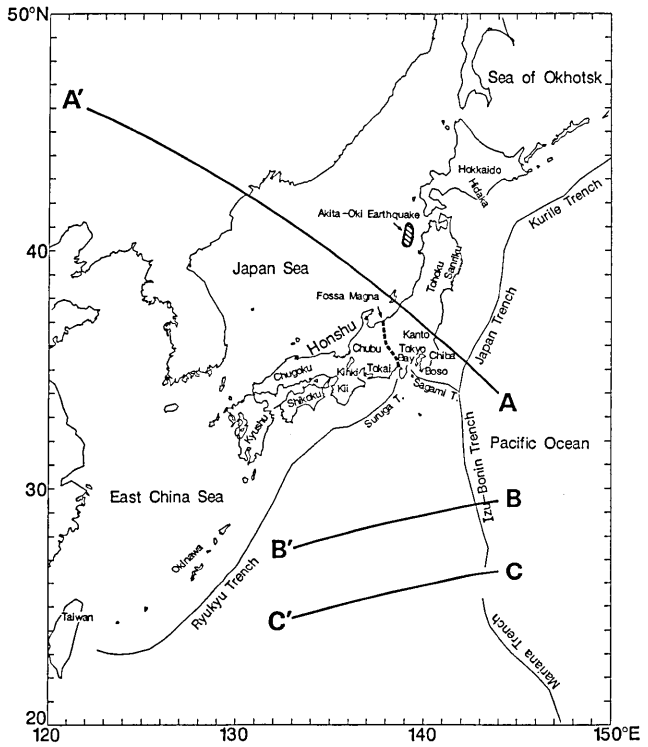

Fig. 1. Index map of the Japanese Islands and their vicinity, which is investigated in this study. Solid lines show the cross sections along which seimic structures are shown in Fig. 10.

regions of the earth. Especially in Japan, many seismologists have succesfully applied their method to reveal the detailed seismic velocity structures on local to regional scale.

On a local scale, for example, HASEMI *et al.* (1984) and OBARA *et al.* (1986) investigated the detailed velocity structure beneath the Tohoku district (see Fig. 1) using travel time data from local earthquakes observed at highly sensitive seismic stations, and found a high velocity Pacific slab and low velocity anomalies above the slab directly beneath active volcanoes. The three-dimensional seismic structure beneath the Kanto-Tokai district was obtained by HORIE and AKI (1982), ISHIDA (1984) and ISHIDA and HASEMI (1988), using local earthquakes, and the high velocity Philippine Sea slab subducting beneath this region was revealed. HIRAHARA (1981) investigated the three-dimensional seismic structure beneath southwest Japan by using 2947 *P*-wave travel time data from the Bulletins of International Seismological Center (ISC), and revealed several remarkable features of the present and past subduction of the Philippine Sea plate. NAKANISHI (1985) applied an approximate inversion

method, called ART (Algebraic Reconstruction Technique), to investigate the three-dimensional seismic velocity structure of the uppermost mantle beneath the Hokkaido-Tohoku region. He used about 7,600 *P*-wave arrival times from the JMA (Japan Meteorological Agency) Bulletin, and a block size of $0.2° \times 0.2° \times 20$ km. He attempted to see time variations of the seismic velocity structure, and found no significant change. There are studies of the three-dimensional structure for other regions in Japan (*e.g.* HIRAHARA *et al.*, 1989; TAKANAMI, 1982; MIYAMACHI and MORIYA, 1984).

Because different data sets, methods, block sizes and initial models were used in these studies, it is very difficult to compare these estimated structures with each other. But we often need a unified velocity model beneath the entire Japanese Islands, for example, when we determine earthquake hypocenters in and near Japan.

On a regional scale, however, there are only two studies of the *P*-wave velocity structure covering the whole Japanese Islands, *i.e.* HIRAHARA (1977) and WATANABE (1977). HIRAHARA (1977) investigated only large-scale heterogeneities using a large block size of $2° \times 2° \times 100$ km. WATANABE (1977) did no resolution analysis, though he used smaller block sizes of $1° \times 1° \times 100$ km and $0.5° \times 0.5° \times 50$ km. It is impossible to discuss how unique the results are without resolution analysis.

Recently it is frequently argued whether the lithospheric slab penetrates into the lower mantle or not. JORDAN (1977) proposed that the lithospheric slab penetrates at least to a depth of 1000 km beneath the Sea of Okhotsk. He obtained a slab model which explains the distribution pattern of travel time residuals on the focal sphere from the deep-focus earthquake of January 29, 1971. The slab model he found has a shear velocity contrast of 5% and extends to a depth of at least 1000 km. By the same method as JORDAN (1977), CREAGER and JORDAN (1984) conclude that the Kuril-Kamchatka slab must penetrate to depths of at least 900-1000 km and the Japan slab deeper than 800 km. CREAGER and JORDAN (1986) applied the residual sphere method to earthquakes in the Mariana and other subduction zones of the Northwest Pacific. They obtained depths of penetration reaching at least 1000 km, 1100-1200 km and 1100 km in the Marianas, Kuril-Kamchatka and Japan subduction zones, respectively, and concluded that the Izu-Bonin slab extends into the lower mantle. SUETSUGU (1988) obtained slab-like high velocity anomalies in the lower mantle beneath the Sea of Okhotsk by inversion of *P*-wave travel times and forward modeling of the teleseismic *P*-wave amplitude.

In this study we attempt to derive a fine three-dimensional seismic

structure beneath the Japanese Islands and their vicinity with resolution analyses using a block size of $0.5^\circ \times 0.5^\circ \times 50$ km. The main purpose of this study is to reveal the structure beneath this region in more detail and to investigate the subducting Pacific and Philippine Sea slabs without any assumption on the configuration of the slab and surrounding mantle. Thus the modeling space is extended to the lower mantle, to a depth of 1200 km, so that it is possible to put some constraints on the problem of slab penetration. A brief report has already been given by KAMIYA *et al.* (1988). Here we give a full description of our result.

2. Data

The total amount of travel time data used here is 103,032. The data are taken from ISC Bulletins. We selected 833 earthquakes observed at more than 50 stations from 1971 to 1983. The source parameters determined by ISC are used as initial input parameters in later calculations. Figure 2 shows the distribution of epicenters with different colors for different hypocentral depth ranges.

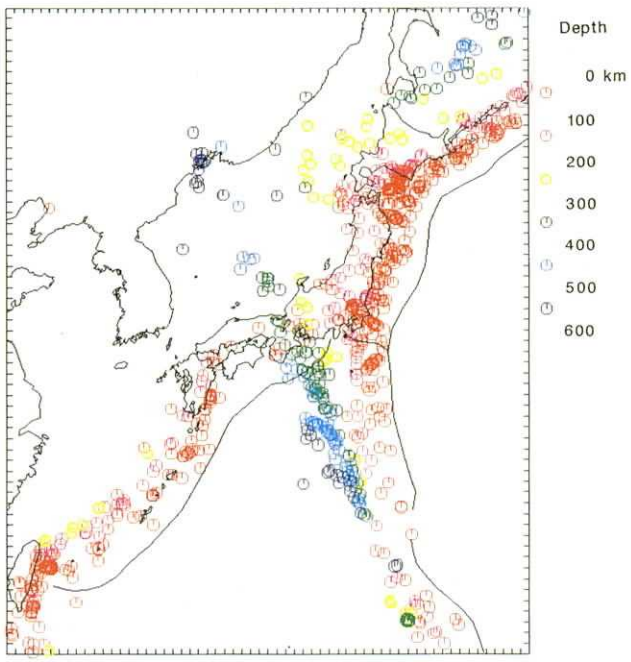

Fig. 2. Distribution of earthquakes used in this study. The focal depth of each event is distinguished in color. The total number of events is 833.

Standard travel times from these earthquakes to each of the stations are computed from the JEFFREYS (1939) velocity model with ellipticity corrections (DZIEWONSKI and GILBERT, 1976) and station-elevation corrections. In the present study, iP and P arrival times are adopted only when the following criteria are satisfied: 1. the absolute travel time residual is less than 5.0 sec, 2. for stations outside the modeling space, epicentral distance ranges from 30° to 100°, and 3. for each station, the number of readings is more than 50. As in HIRAHARA (1977), for stations within the modeling space, the travel time residuals are used as input data without station corrections. For stations outside the modeling space, deviations from the average of travel time residuals at each station are used as input data. The use of these reduced residuals approximately removes the effect of lateral

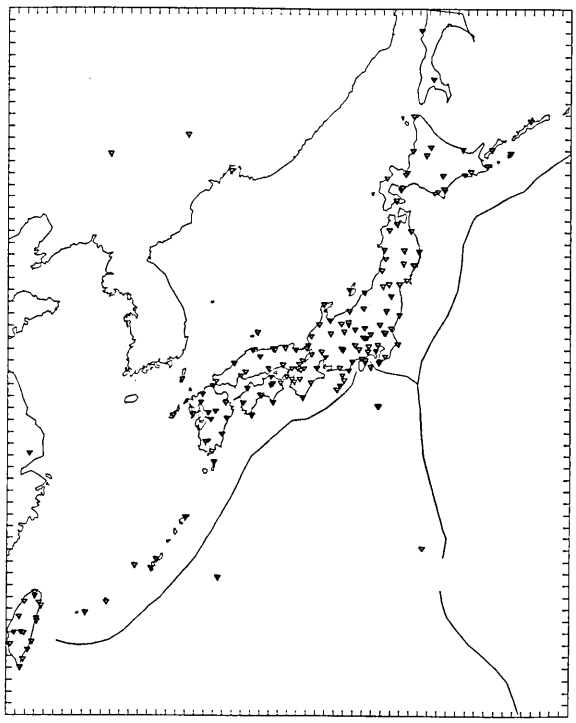

Fig. 3. The stations located within the modeling space. The number of the stations is 173.

heterogeneity outside the modeling space. Figures 3 and 4 show the distribution of stations within the modeling space and that of all stations used in this study, respectively.

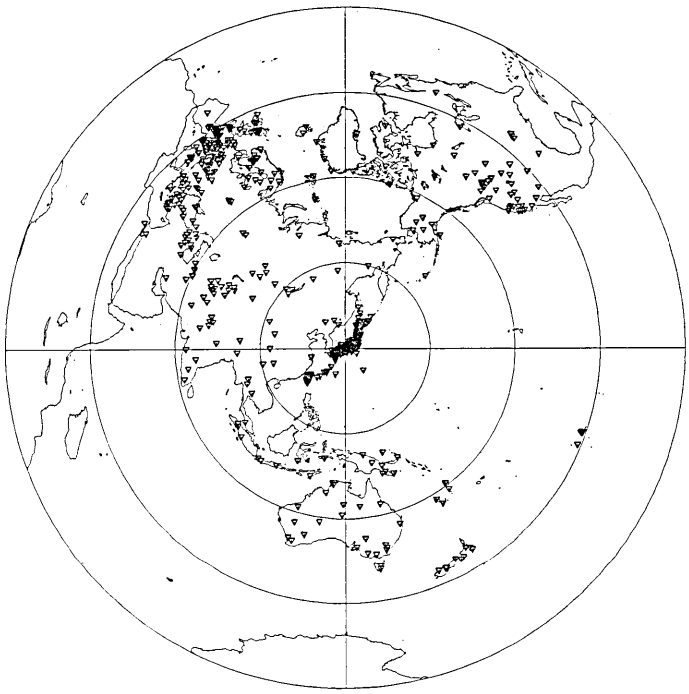

Fig. 4. Lambert equal-area projection centered at 35°N, 135°E, showing the distribution of stations used in this study all over the world. The number of stations is 548.

3. Method

For the modeling space, we take the latitude range of 20°-50°, the longitude range of 120°-150°, and the depth range of 0-1200 km. To reveal fine structure a block size of $0.5° \times 0.5° \times 50$ km (for the uppermost three layers $0.5° \times 0.5° \times 33$ km) is used. Figure 1 shows the area investigated in this study.

The method of analysis used here is ARTB (HIRAHARA 1988), *i.e.*, an ART-type Bayesian reconstruction method which is one of the ART-type iterative tomographic inversion methods, based on the Bayesian optimization criterion. It is possible to estimate a large number of model parameters at the same time because ART-type computation saves memory.

Here, we will briefly describe this method. Let us assume the following linerized equation.

$$\boldsymbol{d} = \boldsymbol{G}\boldsymbol{m}$$

where $\boldsymbol{d}$ and $\boldsymbol{m}$ are the data vector and model vector, respectively.

$\boldsymbol{G}$ is the coefficient matrix. The Bayesian optimization criterion gives the following,

$$(\boldsymbol{d}-\boldsymbol{Gm})^t\boldsymbol{C}_d^{-1}(\boldsymbol{d}-\boldsymbol{Gm})+(\boldsymbol{m}-\boldsymbol{m}_0)^t\boldsymbol{C}_m^{-1}(\boldsymbol{m}-\boldsymbol{m}_0)$$
$$\dashrightarrow \min .$$

where $\boldsymbol{m}_0$ is the initial model vector and $\boldsymbol{C}_d$ and $\boldsymbol{C}_m$ are a priori estimated covariance matrices of the data and model parameter, respectively. It is assumed that $\boldsymbol{C}_d$ and $\boldsymbol{C}_m$ have the following forms

$$\boldsymbol{C}_d=\sigma_d^2\boldsymbol{I}$$

$$\boldsymbol{C}_m=\begin{pmatrix}\sigma_{m1}^2 & & & 0\\ & \ddots & & \\ & & \sigma_{mi}^2 & \\ & & & \ddots \\ 0 & & & \sigma_{mm}^2\end{pmatrix}$$

where σ_d^2 and σ_{mi}^2 are a priori estimates of the covariance for each datum and for the i-th model parameter, respectively, and the matrix $\boldsymbol{I}$ is the $n\times n$ identity matrix. Then the solution of the above equation is written as

$$\boldsymbol{m}-\boldsymbol{m}_0=\boldsymbol{G}^{-g}(\boldsymbol{d}-\boldsymbol{Gm}_0)$$

where

$$\boldsymbol{G}^{-g}=(\boldsymbol{G}^t\boldsymbol{C}_d^{-1}\boldsymbol{G}+\boldsymbol{C}_m^{-1})^{-1}\boldsymbol{G}^t\boldsymbol{C}_d^{-1}$$

The ARTB algorithm is as follows.

$\boldsymbol{u}^{(1)}=\boldsymbol{O}$
$\boldsymbol{m}^{(1)}=\boldsymbol{m}_0$
loop $p=1$ to P (p-th global iteration)
  loop $i=1$ to N (i-th data iteration)
    $k=N\times(p-1)+i$
    $c^{(k)}=\lambda^{(k)}\dfrac{1/\sigma_d(d_i-\langle \boldsymbol{g}_i\boldsymbol{m}^{(k)}\rangle)-u_i^{(k)}}{1+|\bar{\boldsymbol{g}}_i|^2}$
    $\boldsymbol{u}^{(k+1)}=\boldsymbol{u}^{(k)}+c^{(k)}\boldsymbol{e}_i$
    $\boldsymbol{m}^{(k+1)}=\boldsymbol{m}^{(k)}+c^{(k)}\bar{\boldsymbol{g}}_i$
  end loop i
end loop p

Here $\boldsymbol{e}_i$ is the n-dimensional unit vector in which only the i-th component is 1 and the others are zero, and $\boldsymbol{g}_i$, $\bar{\boldsymbol{g}}_i$ and $\bar{\bar{\boldsymbol{g}}}_i$ are defined as follows,

$$\boldsymbol{g}_i=(G_{i1}, \cdots, G_{im})^t$$
$$\bar{\boldsymbol{g}}_i=1/\sigma_d(\sigma_{m1}G_{i1}, \cdots, \sigma_{mm}G_{im})^t$$
$$\bar{\bar{\boldsymbol{g}}}_i=1/\sigma_d(\sigma_{m1}^2G_{i1}, \cdots, \sigma_{mm}^2G_{im})^t$$

$\langle \boldsymbol{g}_i\boldsymbol{m}^{(k)}\rangle$ indicates the inner product of $\boldsymbol{g}_i$ and $\boldsymbol{m}^{(k)}$. Following HIRAHARA (1988), we obtain resolution matrices by ART-type methods. The following standard deviations are assumed for inversion parameters:

$\sigma=0.7$ sec (for data),
$\sigma_i=2.2\%$ (for slowness perturbations),
$\sigma_\lambda=\sigma_\varphi=0.03°$ (for latitude and longitude corrections),
$\sigma_h=3.0$ km (for depth corrections) and
$\sigma_t=0.1$ sec (for origin time corrections).
$\lambda=0.1$ is adopted for the relaxation parameter.

4. Results and Discussions

We solved 833×4 source parameters and 64,197 slowness perturbations for blocks hit by rays simultaneously. Figure 5 shows root-

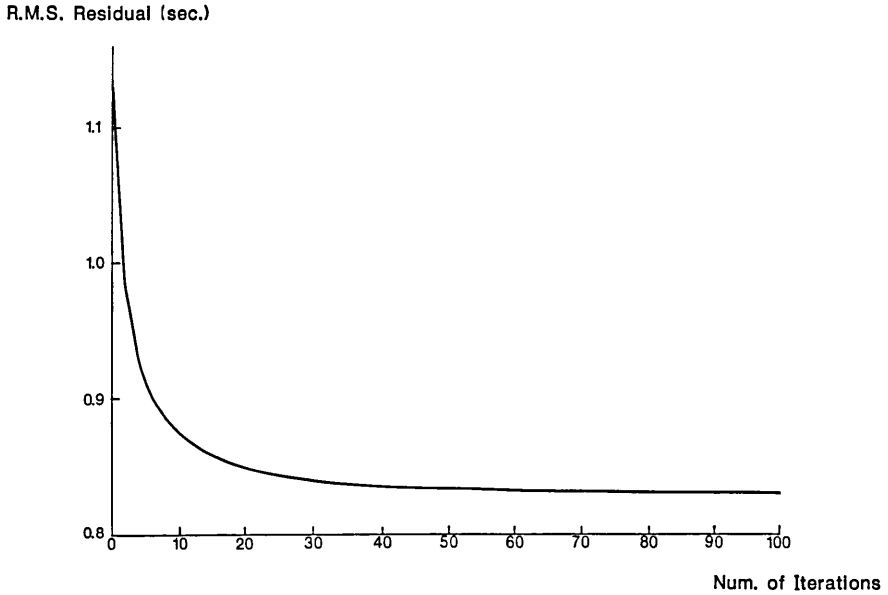

Fig. 5. Root-mean-square residual versus number of global iterations. The root-mean-square residual approximately converged after the 30th iteration.

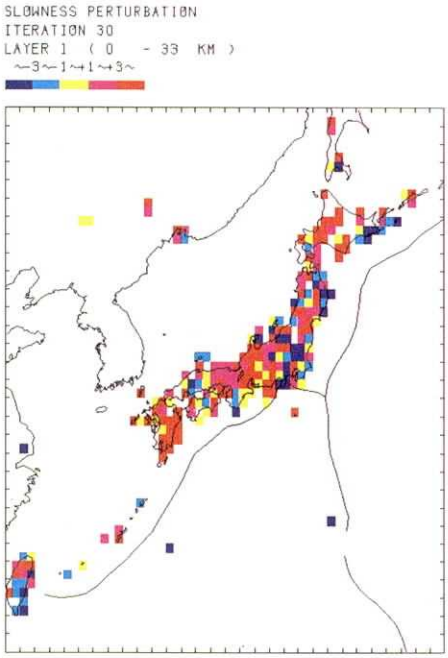

Fig. 6-1

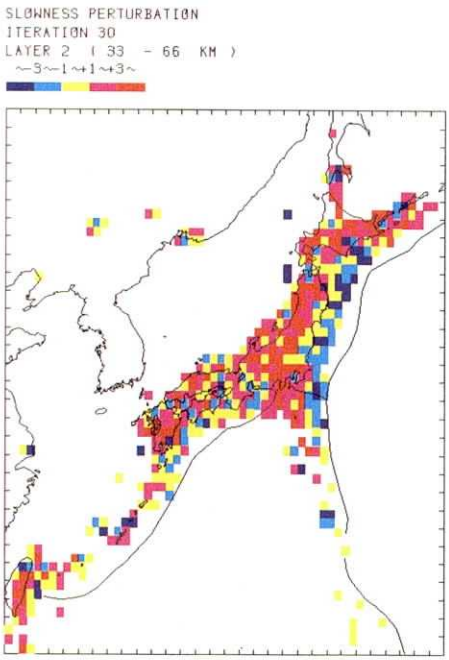

Fig. 6-2

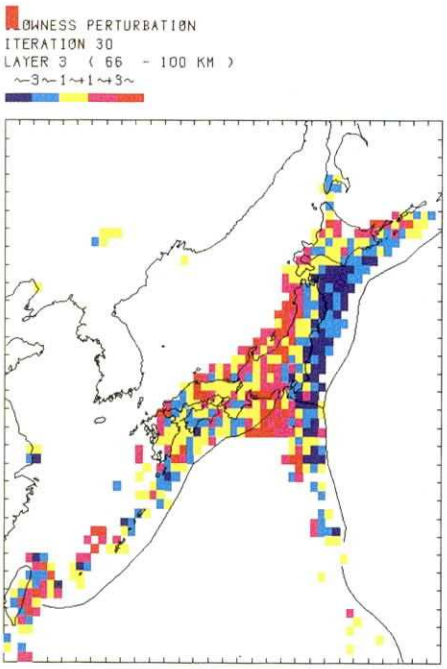

Fig. 6-3

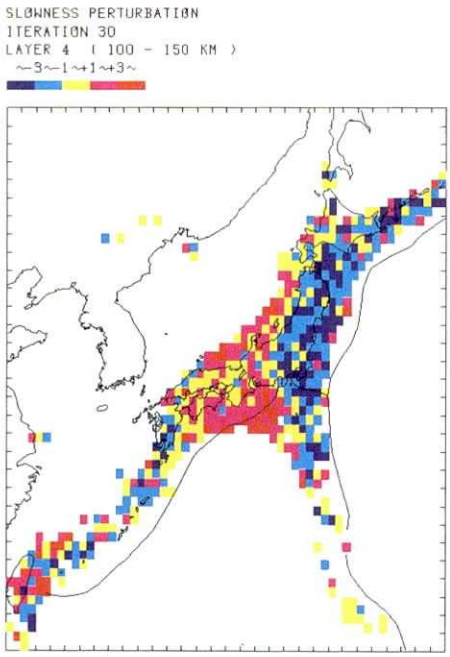

Fig. 6-4

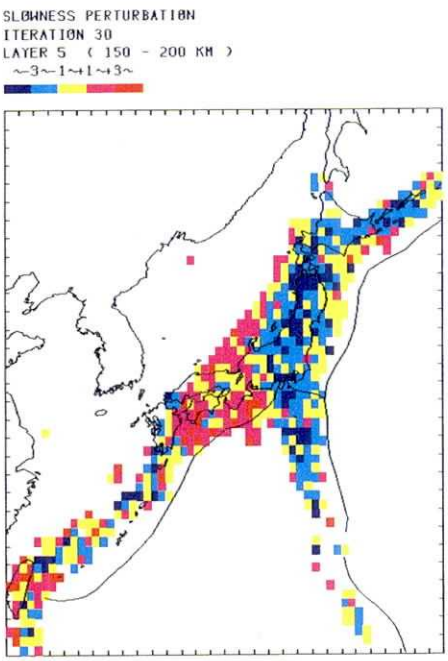

Fig. 6-5

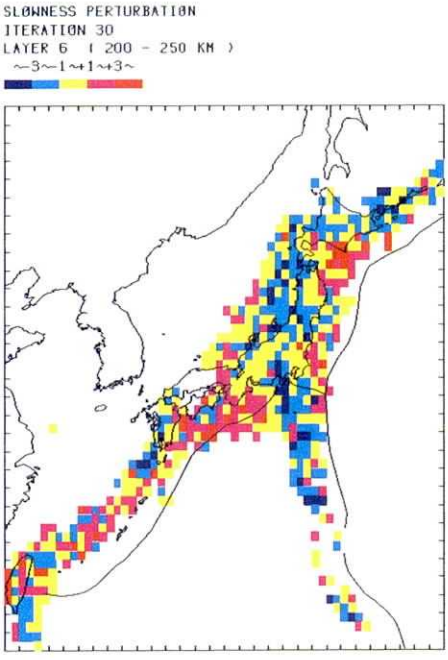

Fig. 6-6

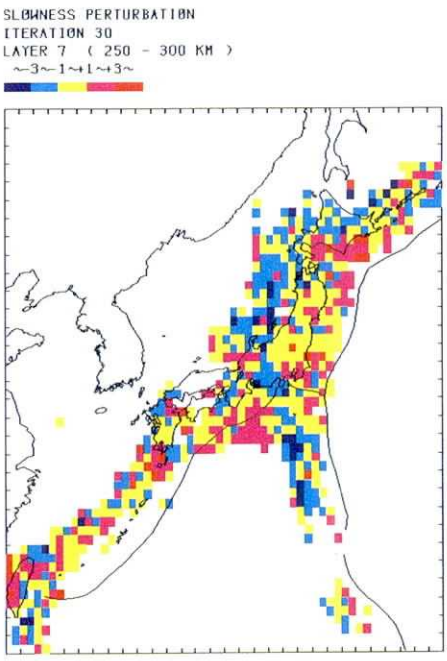

Fig. 6-7

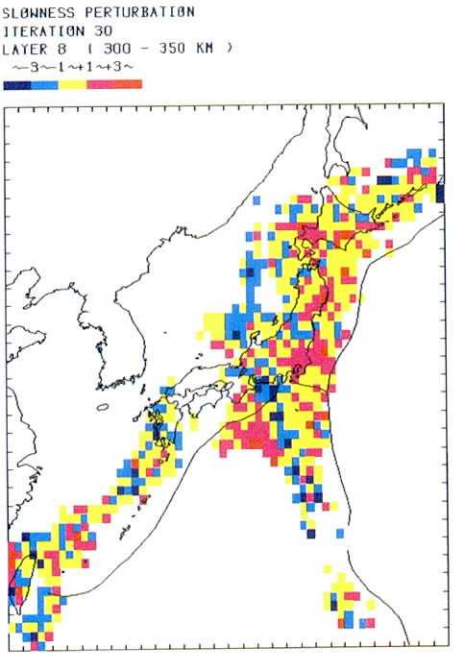

Fig. 6-8

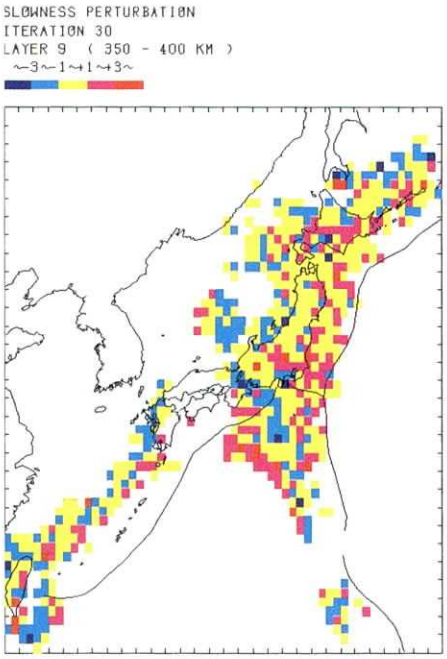

Fig. 6-9

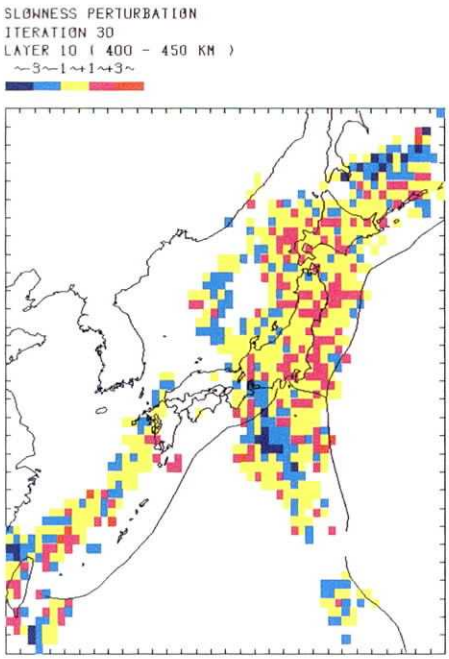

Fig. 6-10

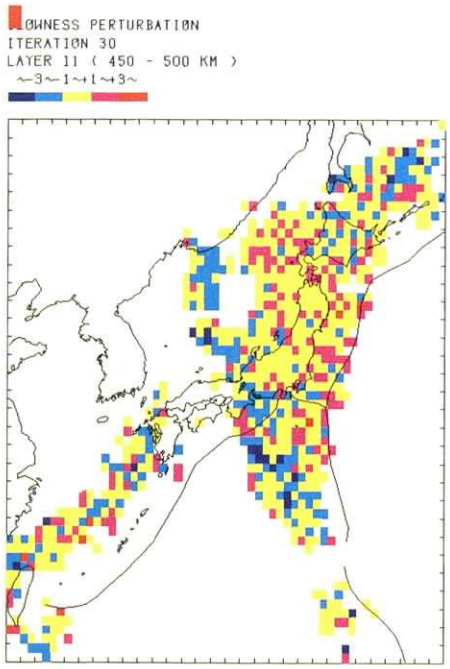

Fig. 6-11

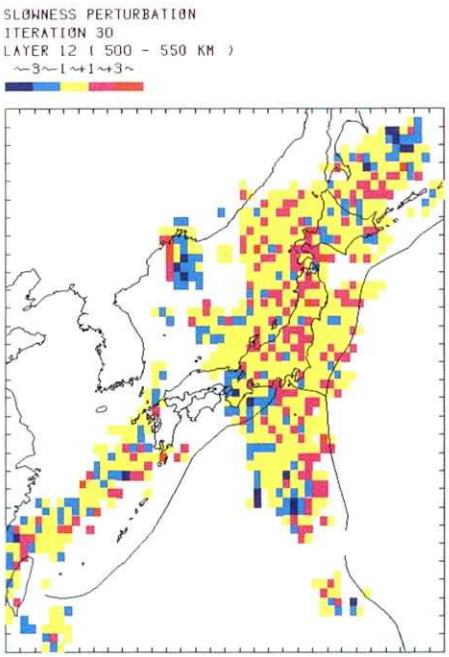

Fig. 6-12

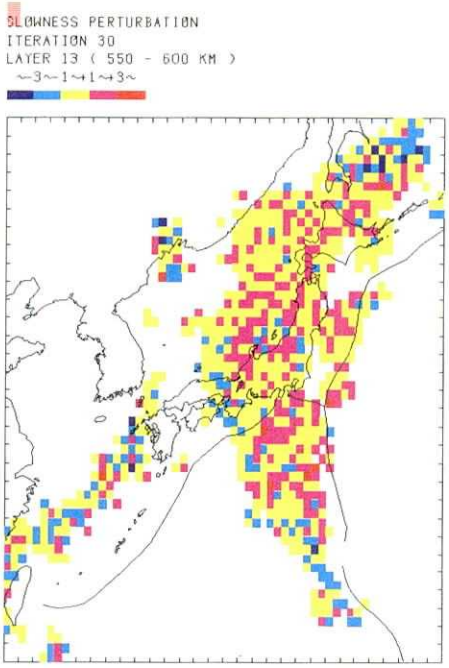

Fig. 6-13

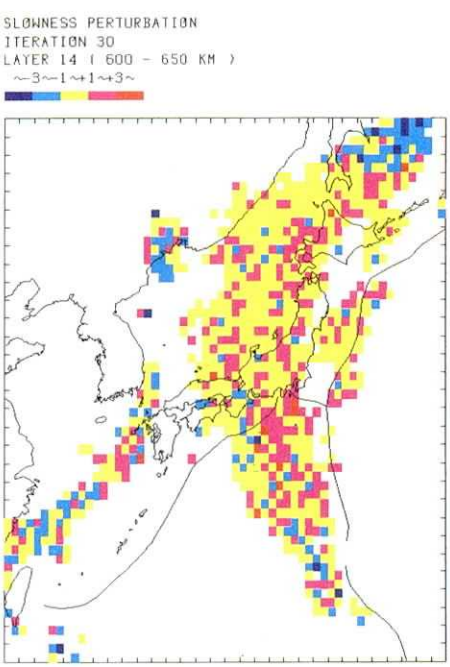

Fig. 6-14

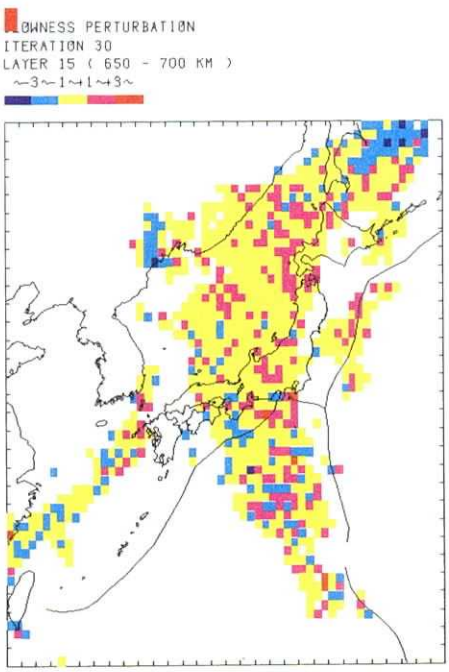

Fig. 6-15

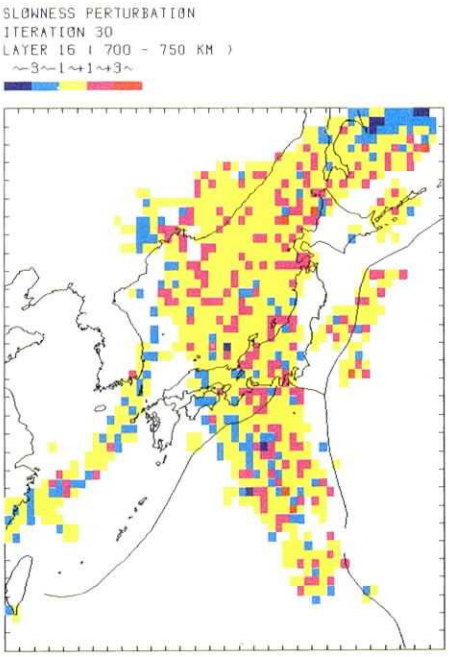

Fig. 6-16

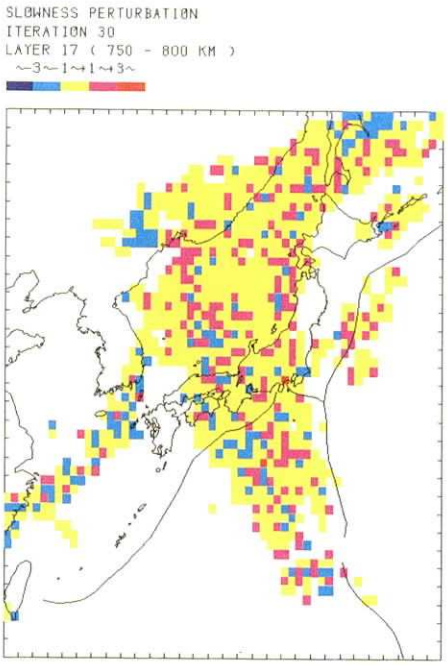

Fig. 6-17

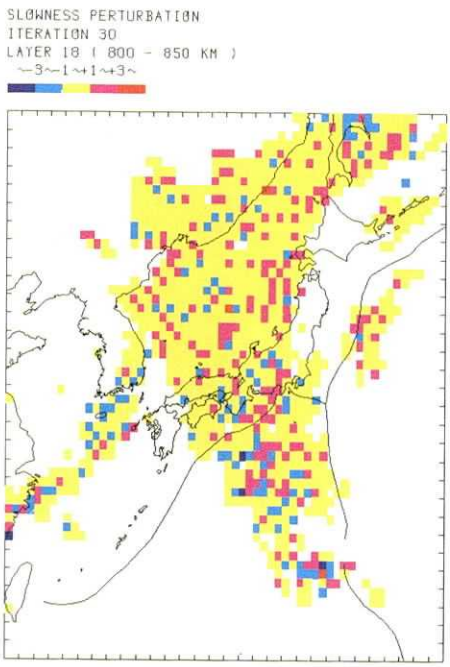

Fig. 6-18

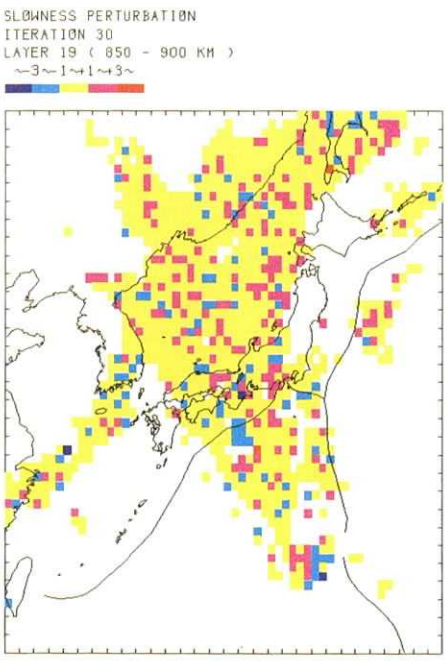

Fig. 6-19

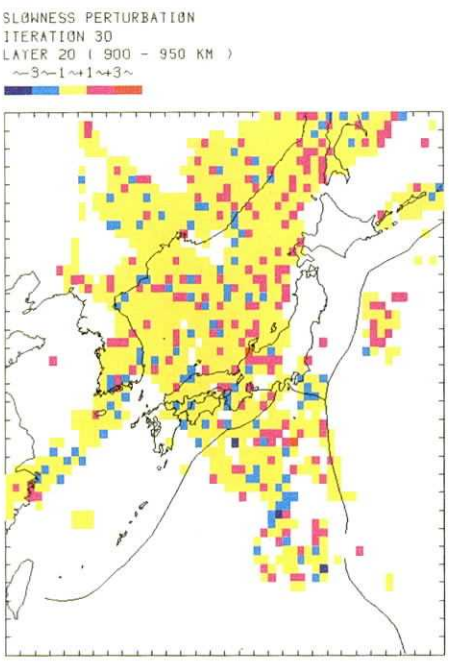

Fig. 6-20

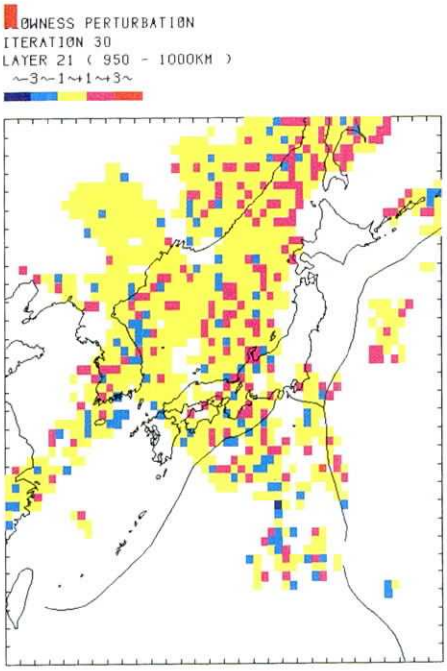

Fig. 6-21

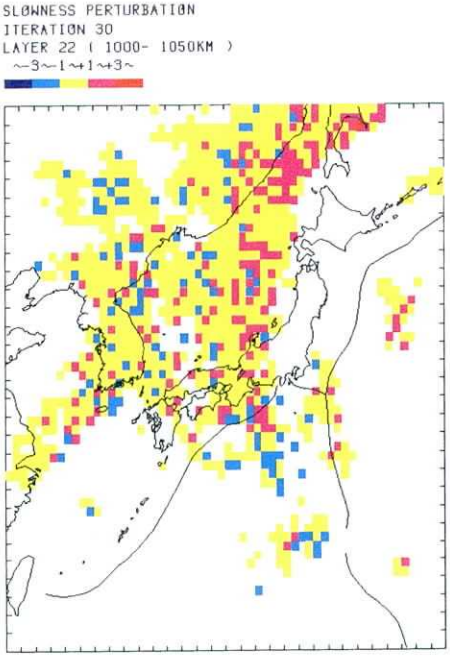

Fig. 6-22

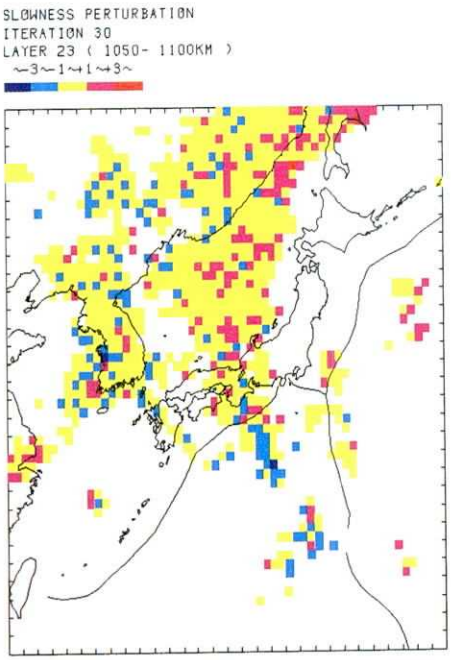

Fig. 6-23

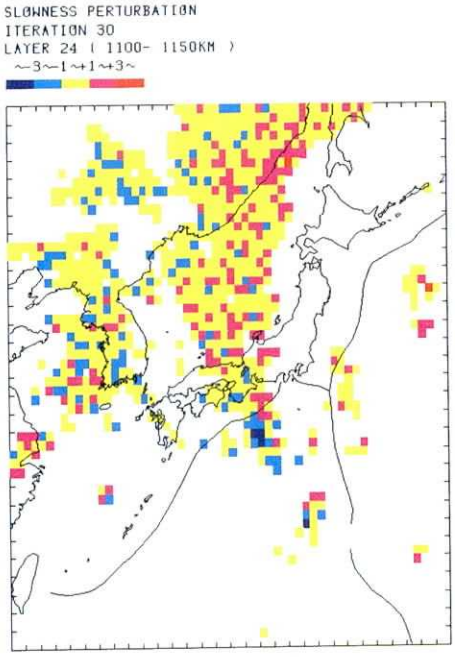

Fig. 6-24

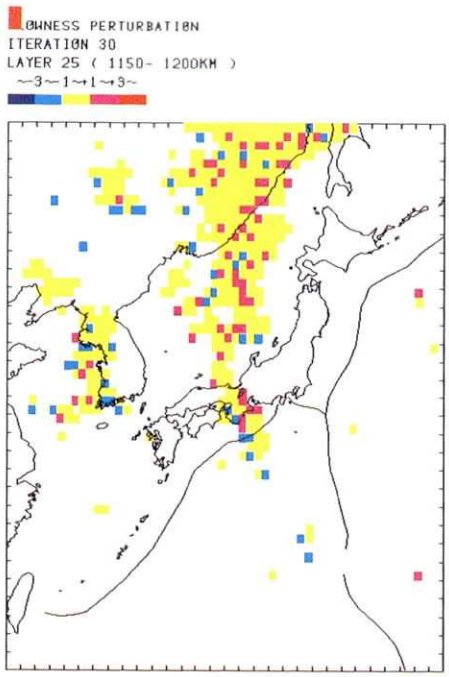

Fig. 6-25

Fig. 6. Results of inversion after the 30th global iteration. The amplitude of slowness perturbations from the model of JEFFREYS (1939) is distinguished in the color of the symbols. Only blocks more than 50 seismic ray penetrations are plotted in each layer. Figs. 6-1 to 6-25 correspond to the results from layer 1 to layer 25, respectively.

mean-square residual of arrival times versus number of global iterations. After about the 30th iteration, the reduction in the residuals is very small. So, we show the results after the 30th iteration in later discussions. Root-mean-square residuals before and after are 1.13 sec and 0.83 sec, respectively. The results are shown in Fig. 6. Figure 7 shows the Wadati-Benioff zone. The distributions of gravity anomalies (HAGIWARA, 1967) and heat flow (YUHARA, 1973) are shown in Figs. 8 and 9, respectively. The obtained velocity structure can be compared with these figures.

Layer 1 (0-33 km, Fig. 6-1)

The obtained structure in layer 1 partly includes the effect of local structure close to the stations within the modeling space, because no station corrections are considered for those stations.

In the Hokkaido district, high velocity anomalies are found only along the Pacific coast of the eastern part. On the other hand, it appears that low velocity anomalies occur not only near volcanoes but almost all of Hokkaido. The high velocity region corresponds to positive

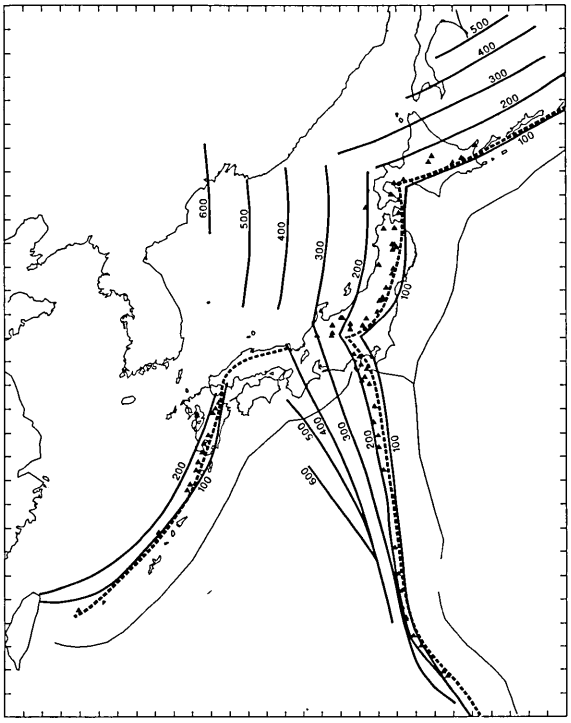

Fig. 7. Contour map of the Wadati-Benioff zone. Solid lines show the Wadati-Benioff zone. Broken lines show volcanic fronts. Triangles show active volcanoes.

Bouger anomaly distribution both of short and long wavelength (Figs. 8a and 8b). However, the low velocity anomalies do not correspond to observed Bouger anomalies.

In the Tohoku district, the low velocity areas in the central and southern parts correspond to the distribution of volcanoes (Fig. 7). This is consistent with previous studies of three-dimensional seismic velocity structure (HASEMI *et al.*, 1984; OBARA *et al.*, 1986) and attenuation structure (HASHIDA and SHIMAZAKI, 1987). The high and low velocity anomalies correspond to positive and negative Bouger anomalies of short wavelength, respectively. This represents heterogeneity in the crust in this district, as suggested by OBARA *et al.* (1986).

In the Kanto district, low velocity anomalies are found in and around Tokyo Bay, and high velocity anomalies in northern Kanto, Izu Peninsula, and Boso Peninsula. This feature is consistent with the previous studies by HORIE and AKI (1982), and ISHIDA (1984), but not with that by HIRAHARA (1981). And it also corresponds very well to the distribution of Bouger anomalies of short wavelength; that is low

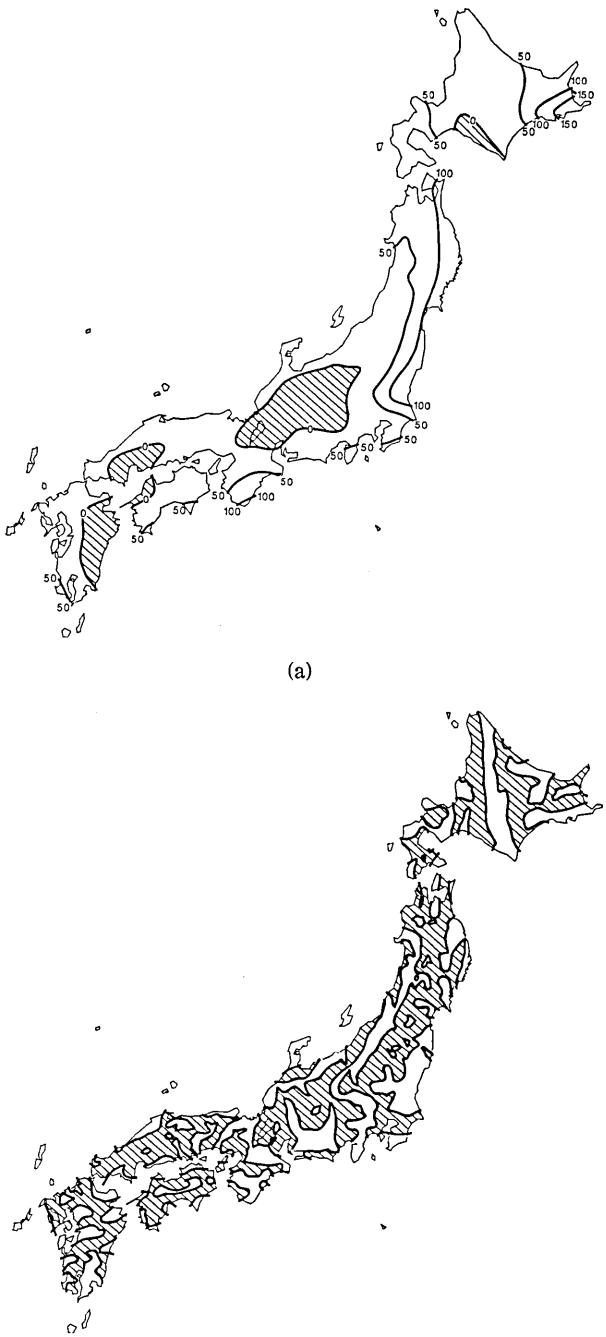

Fig. 8. Bouger anomaly distribution of long (a) and short (b) wavelength in Japan. Hatched regions show negative Bouger anomalies (after HAGIWARA, 1967). Contour interval is 50 mgal.

velocity anomalies correspond to negative Bouger anomalies and high velocity anomalies to positive ones. The low velocity anomalies occur in thick sedimentary layers covering Tokyo Bay, and high velocity anomalies correspond to crust with a higher density.

Across the Fossa Magna, the remarkable geological boundary between northeast and southwest Japan, a velocity contrast appears. There exist relatively high veocity anomalies on the eastern side and low velocity on the western side. This velocity contrast has been suggested from explosion studies (OKADA *et al.*, 1979). The low velocity anomalies in the Chubu region west of the Fossa Magna correspond to negative Bouger anomalies. The low velocity anomalies probably reflect a thick upper crustal layer with low velocity and low density, because it is known that the crust is not so thick, less than 30 km, from explosion seismic observations (AOKI *et al.*, 1972).

The low velocity anomalies extend through Kinki to eastern Chugoku. This feature is not consistent with previous studies of seismic velocity (*e.g.*, HIRAHARA, 1981) and attenuation (HASHIDA, 1987) structure. It is also inconsistent with Bouger anomalies, as the negative Bouger anomalies of long wavelength in the Kinki district don't extend westward. High velocity anomalies are found in the southwestern part of the Kii Peninsula. These anomalies were also found by HIRAHARA (1981), they correspond to positive Bouger anomalies of long and short wavelength.

In the Kyushu district and northern Taiwan, low velocity anomalies are found. Several active volcanoes exist at the northern tip of Taiwan (CHEN and WU, 1971) and on Kyushu region. Low velocity anomalies in this region are considered manifestations of the volcanism.

Layer 2 (33-66 km, Fig. 6-2)

In this layer, high velocity anomalies appear from the Hokkaido to Kanto regions along the Pacific coast and from the Tokai to Okinawa regions along the Philippine Sea coast. These anomalies are thought to reflect the Pacific and Philippine Sea slabs, respectively, because seismic activities are found in these high velocity regions. The Philippine Sea slab is not so clear as the Pacific slab in Fig. 6-2. This is partly because the Philippine Sea slab is thinner, about 30 km (*e.g.* HIRAHARA, 1981), than the Pacific slab. Also, the small number of stations along the Philippine Sea coast, especially along the Ryukyu Trench, makes it difficult to obtain a clear picture of the slab. Another high velocity anomaly is found beneath the source area of the 1983 Akita-Oki earthquake. SATO and KOSUGA (1987) estimated high P_n velocity (8.20-8.27 km/sec) in the area, using arrival time data of aftershocks. The result of the present study is consistent with the estimated

high P_n velocity.

In northeastern Japan, low velocity anomalies are mostly distributed west of the volcanic front (Fig. 7), except south of the Kurile Islands, the Hidaka region, the northern part of Sanriku and the southern part of Kanto. In the southern Kurile Islands, it seems that low velocity anomalies lie beneath the high velocity blocks in layer 1. Resolution analyses show that the low velocity anomalies are not influenced so much by the high velocity blocks lying above. Thus these lows are probably not due to an artifact but are existing features of unknown origin. In the Hidaka region, the anomalies are thought to reflect the thick crust and low P_n velocity. This is supported by previous studies (TAKANAMI, 1982; MIYAMACHI and MORIYA, 1984), an explosion study (OKADA *et al.*, 1973), and the negative Bouger anomalies of long wavelength. In southwestern Japan, low velocity anomalies are distributed west of the volcanic front, except for the southwestern part of Chugoku, the western part of Shikoku and the eastern part of Kyushu. The low velocity anomalies in these regions are consistent with the negative Bouger anomalies of long wavelength. Low velocity anomalies are found in most parts of Taiwan. This feature is also consistent with the negative Bouger anomalies.

Layers 3 to 7 (66-300 km, Fig. 6-3 to Fig. 6-7)

In these layers, high velocity anomalies correlate well with hypocenters of earthquakes from the Kuriles to the Izu-Bonin Islands, parallel to the Kurile, Japan, and Izu-Bonin Trenches, and also from Kyushu to Taiwan, parallel to the Ryukyu Trench. The amplitude of these high velocity anomalies is about 2-5%. This indicates that they reflect the Pacific and Philippine Sea slabs. These high velocity anomalies corresponding to the slabs are clearer than those in layer 2. This is because more seismic rays penetrate these high velocity blocks. However, high velocity anomalies no longer appear in southwestern Honshu and Shikoku below layer 3. In this region, it is recognized that the Philippine Sea slab does not reach to these depths as was suggested by HIRAHARA (1981). Almost no seismic activities exist at these depths.

Low velocity anomalies are found overriding the Pacific and Philippine Sea slabs, especially beneath the Philippine Sea and the southeast rim of the Japan Sea above the Pacific slab. The amplitude of these low velocity anomalies is about 2-4%. ANDERSON and SPETZLER (1970) used the Eshelby-Walsh theory and calculated the compressional and shear velocities in a solid matrix with penny-shaped melt zones as a function of melt concentration and aspect ratio of the melt zones. Using their result, low velocity anomalies of 2-4% can be explained

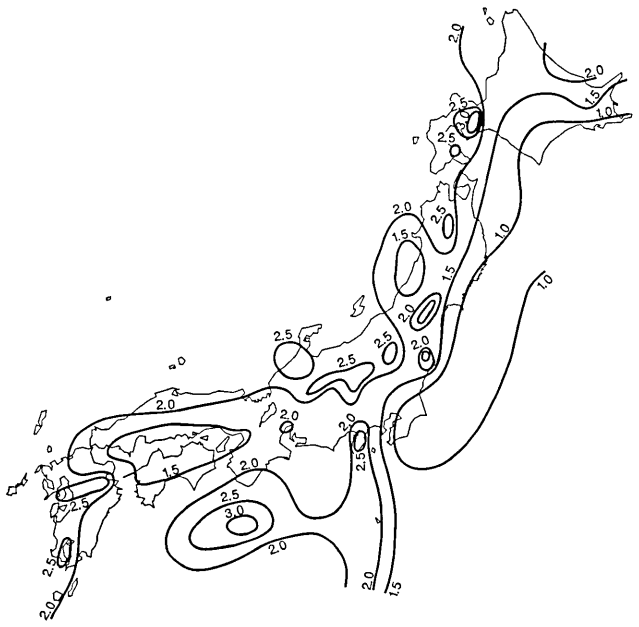

Fig. 9. Contour map of heat flow in Japan (after YUHARA, 1973). Values are shown in HFU.

by 1% melt if the aspect ratio is 10^{-2}. And the velocity contrast between the slab and the overriding mantle in this study is about 4-7%, which is consistent with previous studies (*e.g.* MATSUZAWA *et al.*, 1986).

Low velocity anomalies cannot be seen beneath the Kinki and Chugoku regions above the Pacific slab. In these regions the observed heat flow is relatively low (Fig. 9).

Layers 8 to 14 (300-650 km, Fig. 6-8 to Fig. 6-14)

High velocity anomalies are found corresponding to the Pacific slab which is estimated from earthquake hypocenters. The anomalies are not continuous from the Kurile to Izu-Bonin arcs, but divided into several parts. The areas of high velocity anomalies become smaller as the layer becomes deeper. This is because the number of deep focus earthquakes used is less than that of shallow or intermediate-depth ones, and deep earthquakes occur only in a few specific regions. Therefore, many seismic rays penetrate only a few blocks.

Low velocity anomalies are found overriding the Pacific slab beneath the Philippine Sea to a depth of 450 km, and beneath the Japan Sea to a depth of 650 km. From 450 km to 650 km the low velocity anomalies beneath the Japan Sea appear very clearly, though they are obscure

above this depth range. SUYEHIRO and SACKS (1983) investigated *P*-wave travel time residuals for local intermediate and deep focus earthquakes, and concluded that there are lower velocity regions below a depth of about 300 km and above the deepest earthquakes beneath the southern Okhotsk Sea and the western Japan Sea. Our velocity model obtained here is consistent with their result.

Running parallel to the Ryukyu Trench, high velocity anomalies are found to a depth of 600 km. These high velocity anomalies, which are not accompanied by seismic activity, shall be discussed later.

Layers 15 to 25 (650-1200 km, Fig. 6-15 to Fig. 6-25)

No earthquake occurs deeper than 650 km within the Pacific slab *e.g.* YOSHII, 1979). Our results, however, show that the high velocity anomalies extend beneath the area west of Vladivostok from 650 km to 1200 km, and beneath the west of the Izu-Bonin Trench to a depth of 850 km, well beyond the termination of seismic activity. In a previous paper (KAMIYA *et al.*, 1988), we have briefly discussed high velocity anomalies beneath the Japan Sea. In this paper, we shall discuss these in detail using three cross sections of AA′, BB′ and CC′ (Fig. 10), whose locations are indicated in Fig. 1.

Vertical section across the Japan Trench

In cross section AA′ (Fig. 10a), high velocity anomalies are found dipping westward with a dip angle of about 30° in the upper mantle. We conclude that this high velocity zone corresponds to the Pacific slab, because hypocenters of intermediate-depth and deep events lie within the high velocity anomalies.

At a depth of 600 km, seismic activity ends and the dip of the high velocity zone changes from 30° to 50°. Beyond this depth, the high velocity zone further continues down to a depth of 1200 km.

This feature is similar to the result of CREAGER and JORDAN (1986), although their dip angle of 55° in the lower mantle is slightly greater than that of the present study. This difference may be attributed to the omission of three-dimensional ray tracing in our analysis, because the inclusion of high velocity anomalies causes the rays to have smaller take-off angles, hence the dip angle becomes larger.

This high velocity zone seems to be the Pacific slab penetrating to the lower mantle. However, there exists a possibility that this slab-like high velocity anomaly may be the seep caused by artificial spreading of high velocity in the upper mantle because of the lack of resolution.

By resolution analyses it is confirmed that there exist high velocity anomalies in the lower mantle. The resolution kernel of the target block is shown by the asterisk in Fig. 10a. As seen from Fig. 11,

showing an enlarged map of this resolving kernel along the same cross section, the solution is unresolved in the dip direction, well-resolved in the direction perpendicular to it. The resolving kernel has only small values in the upper mantle. Accordingly, we can say positively that the high velocity anomaly in the target block is little influenced by those in the upper mantle. Even if we move the target to a shallower depth, this conclusion holds, for example, for a target in layer 15 (depth of 650–700 km). However, the diagonal values of the resolution kernel are relatively low in the lower mantle, and the values of velocity anomalies obtained are possibly underestimated.

These high velocity anomalies in the lower mantle are considered to be the penetrating slab (*e.g.* CREAGER and JORDAN, 1986), while they are also considered to be thermal coupling between convections within upper and lower mantles, without penetrating slab into the lower mantle (*e.g.* HONDA, 1987). In this study it is impossible to deny either of these conclusions.

In this profile, it appears that deep earthquakes occur in the low velocity anomalies in a depth range of 500–600 km, which was also suggested by HIRAHARA (1977) and ZHOU and CLAYTON (1988).

Vertical section across the Izu-Bonin Trench

Cross sections BB′ and CC′ (Figs. 10b and 10c) reveal the Pacific slab subducting from the Izu-Bonin Trench. From the trench to a depth of 400 km, the dip of high velocity anomalies increases downward. The high velocity anomalies are well correlated with the seismicity in the upper mantle, *i.e.*, the Wadati-Benioff zone, though it is rather unclear

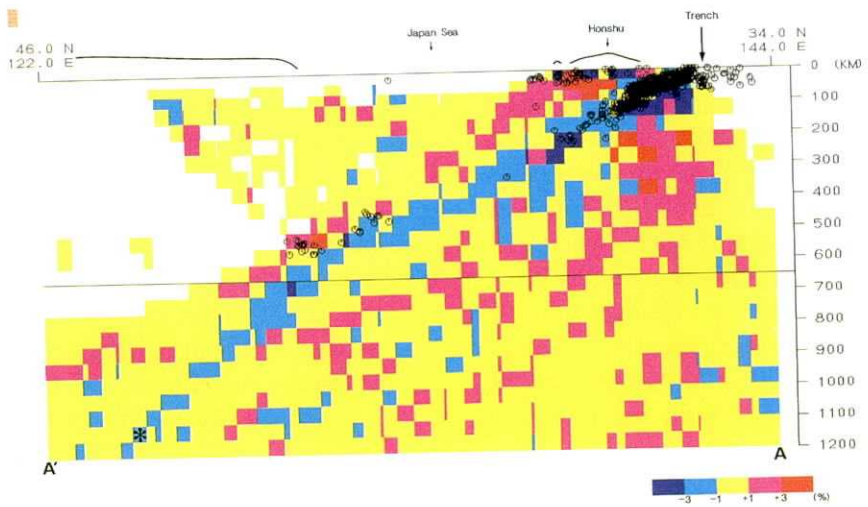

Fig. 10a

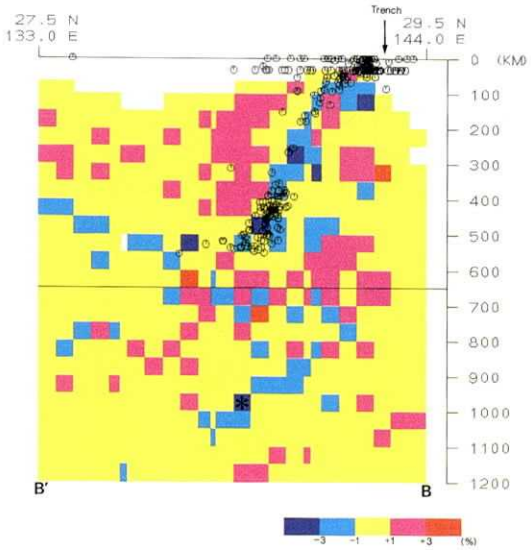

Fig. 10b

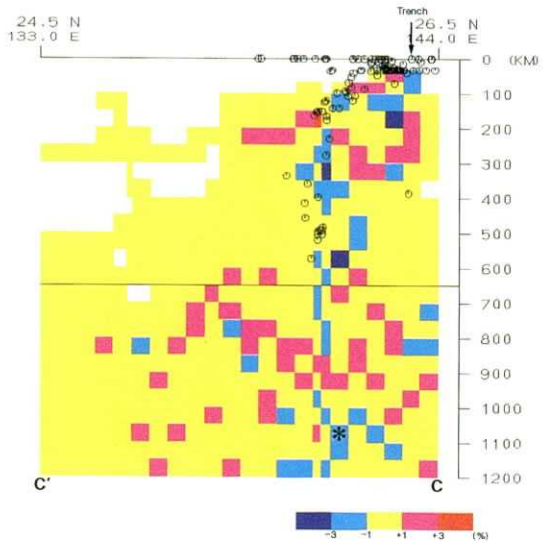

Fig. 10c

Fig. 10. Profiles of seismic structure of three cross sections in Fig. 1. Slowness perturbations of all solved blocks are distinguished in color. They also shown hypocenters whose magnitude is more than 1.0 by the ISC which occurred within 1.0 degree on both sides of each section projected onto the vertical cross section. The locations of the cross sections of Figs. 10a, 10b and 10c correspond to AA′, BB′ and CC′ in Fig. 1, respectively. The block asterisked in each profile is the target of resolution analysis.

at shallow depths in section CC'.

For cross section BB' (Fig. 10b), the high velocity region becomes almost horizontal at a depth of 500-550 km. This suggests that the Pacific slab is bent westward at this depth. Looking at the resolving kernel of the target block shown by the asterisk in Fig. 10b, strong correlation is not found with the other blocks in the same or near-by layers. And the deep seismicity extends not downward but westward in this layer. Moreover, high seismicity is found in the high velocity region in the depth range from 350 km to 550 km, where the slab appears to be bent.

However, in another cross section CC' (Fig. 10c), the southern

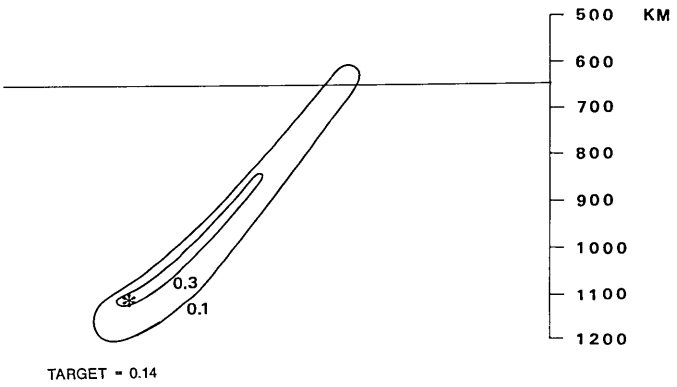

Fig. 11a

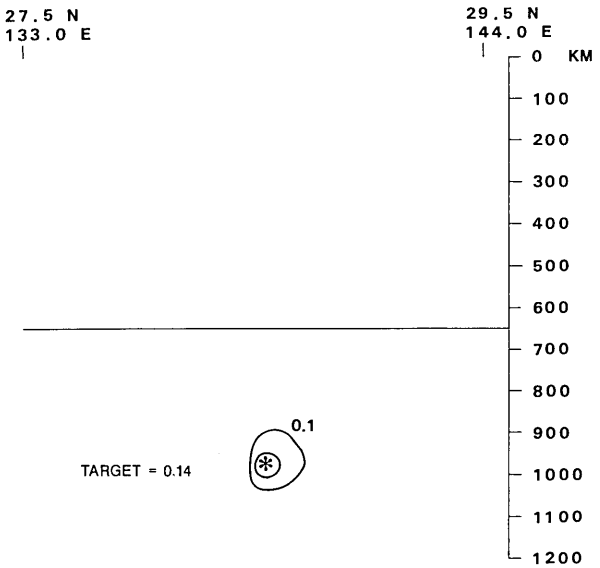

Fig. 11b

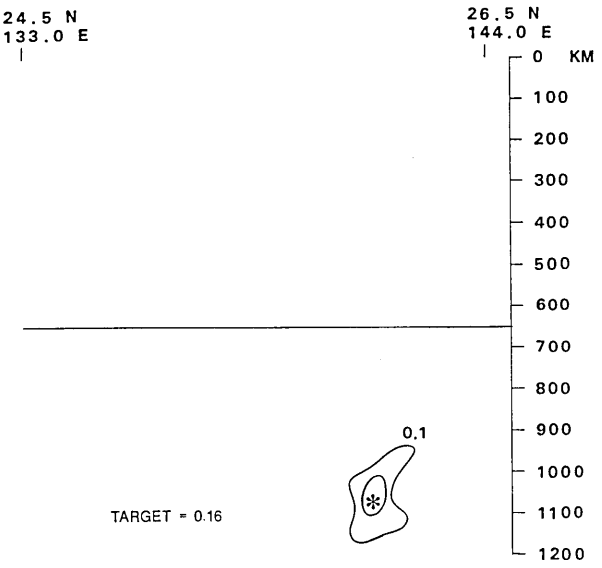

Fig. 11c

Fig. 11. Enlarged map of resolving kernel for the target block shown by the asterisk in Fig. 10. Contour lines indicate values of off-diagonal elements for the corresponding column of the resolution matrix, which is normalized by the diagonal element.

profile of the Izu-Bonin region, the high velocity zone is not horizontal at a depth of 550 km, but it appears to extend vertically to 850 km. No concentration of earthquakes suggesting that the slab bends as in cross section BB′ is found in this profile.

CREAGER (1984) analyzed residual spheres of travel times for five earthquakes near the Bonin Islands at latitude about 26°N, near the cross section CC′ in this study, and asserted that the slab penetrates into the lower mantle in this region. North of these events, the residual sphere patterns are very complicated and a complicated mode of subduction is suggested (CREAGER, personal communication). These results are consistent with the velocity structures in this study.

Therefore, along the Izu-Bonin Trench the slab may be fingering and extend in various directions at a depth of 500-550 km.

5. Conclusions

Detailed features of lateral heterogeneity in the upper mantle beneath the Japanese Islands has been revealed by applying the inversion technique of ARTB. High velocity zones corresponding to the Pacific and Philippine Sea slabs are well defined.

In the lower mantle, slab-shaped high velocity anomalies are found

beyond the termination of the Wadti-Benioff zone along the Japan and Izu-Bonin Trenches. By resolution analyses, it is ascertained that slab-like anomalies are actually present in the lower mantle and that they are not seep caused by spurious apparent spreading of the high velocity anomaly of the slab in the upper mantle. However, it is impossible to see how far the slab-like anomalies continue downward, because most of the ray paths in the high velocity region have almost the same direction and the obtained high velocity region extends along the ray paths.

Two probable causes are considered for the high velocity anomalies in the lower mantle. One is a penetrating slab (*e.g.*, CREAGER and JORDAN, 1986). Another is thermal coupling between convection within the upper and lower mantles, without penetration of a slab into the lower mantle (*e.g.* HONDA, 1987).

On the slab descending from the Izu-Bonin Trench, if the slab-shaped high velocity anomalies are penetrating, the slab is considered to be fingering. At latitude about 26°N, the slab-shaped high velocity anomaly penetrates vertically into the lower mantle. On the other hand, at latitude about 29°N, the high velocity anomaly is bent horizontally westward at a depth of 500–550 km. Corresponding to this high velocity anomaly, the deep seismicity exists in the depth range from 350 km to 550 km and it extends westward at the depth of 500 km.

Acknowledgments

We are very grateful to Prof. K. Shimazaki for his advice and useful discussions throughout this study. We would like to thank Dr. K. C. CREAGER for his valuable advice and discussions. We also would like to thank many members of the Earthquake Research Institute for useful discussions.

References

AKI, K. and H. K. LEE, 1976, Determination of three-dimensional velocity anomalies under a seismic array using first *P* arrival times from local earthquakes. 1. A homogeneous initial model, *J. Geophys. Res.*, **81**, 4381–4399.

AKI, K., A. CHRISTOFFERSSON and E. S. HUSEBYE, 1977, Determination of the three-dimensional seismic structure of the lithosphere, *J. Geophys. Res.*, **82**, 277–296.

ANDERSON, D. L. and H. SPETZLER, 1970, Partial melt and the low-velocity zone, *Phys. Earth Planet. Inter.*, **4**, 62–64.

AOKI, H., T. TADA, Y. SASAKI, T. OOIDA, I. MURAMATU, H. SHIMAMURA and I. FURUYA, 1972, Crustal structure in the profile across central Japan as derived from explosion seismic observations, *J. Phys. Earth*, **20**, 197–223.

CHEN, C. H., and Y. J. WU, 1971, Volcanic geology of the Tatun geothermal area, northern Taiwan, *Proc. Geol. Soc. China*, **18**, 59–72.

CREAGER, K. C., 1984, Geometry, velocity structure, and penetration depths of descending slabs in the western Pacific, *Ph. D. dissertation, Univ. of Calif.*, San Diego, La Jolla.

CREAGER, K. C. and T. H. JORDAN, 1984, Slab penetration into the lower mantle, *J. Geophys. Res.*, **89**, 3031-3049.

CREAGER, K. C. and T. H. JORDAN, 1986, Slab penetration into the lower mantle beneath the Mariana and other island arcs of the Northwest Pacific, *J. Geophys. Res.*, **91**, 3573-3589.

DZIEWONSKI, A. M. and F. GILBERT, 1976, The effect of small, aspherical perturbation on travel times and a re-examination of the corrections for ellipticity, *Geophys. J. R. Astr. Soc.*, 44, 7-17.

HAGIWARA, Y., 1967, Analyses of gravity values in Japan, *Bull. Earthq. Res. Inst., Univ. Tokyo*, **45**, 1091-1228.

HASEMI, A. H., H. ISHII and A. TAKAGI, 1984, Fine structure beneath the Tohoku District, northeastern Japan arc, as derived by an inversion of *P*-wave arrival times from local earthquakes, *Tectonophysics*, **101**, 245-265.

HASHIDA, T., 1987, Determination of three-dimensional attenuation structure and source acceleration by inversion of seismic intensity data: Japanese Islands, *Bull. Earthq. Res. Inst., Univ. Tokyo*, **62**, 241-287.

HASHIDA, T. and K. SHIMAZAKI, 1984, Determination of seismic attenuation structure and source strength by inversion of seismic intensity data: Method and numerical experiments, *J. Phys. Earth*, **32**, 299-316.

HASHIDA, T. and K. SHIMAZAKI, 1987, Determination of seismic attenuation structure and source strength by inversion of seismic intensity data: Tohoku District, northeastern Japan arc, *J. Phys. Earth*, **35**, 67-92.

HIRAHARA, K., 1977, A large-scale three-dimensional seismic structure under the Japan Islands and the Sea of Japan, *J. Phys. Earth*, **25**, 393-417.

HIRAHARA, K., 1981, Three-dimensional seismic structure beneath southwest Japan: the subducting Philippine Sea plate, *Tectonophysics*, **79**, 1-44.

HIRAHARA, K., 1988, Detection of three-dimensional velocity anisotropy, *Phys. Earth Planet. Inter.*, **51**, 71-85.

HIRAHARA, K., A. IKAMI, M. ISHIDA and T. MIKUMO, 1989, Three-dimensional *P*-wave velocity structure beneath Central Japan: low-velocity bodies in the wedge portion of the upper mantle above high-velocity subducting plates, *Tectonophysics*, **163**, 63-73.

HONDA, S., 1987, Two-layer convection with a soft boundary-slab penetration and mantle convection (in Japanese with English abstract), *Zisin (J. Seismol. Soc. Jpn.), Ser. 2*, **40**, 575-592.

HORIE, A. and K. AKI, 1982, Three-dimensional velocity structure beneath the Kato District, Japan, *J. Phys. Earth*, **30**, 255-281.

ISHIDA, M., 1984, The spatial distribution of earthquake hypocenters and the three-dimensional velocity structure in the Kanto-Tokai District, Japan, *J. Phys. Earth*, **32**, 399-422.

ISHIDA, M. and A. H. HASEMI, 1988, The three-dimensional fine velocity structure and hypocentral distribution of earthquakes beneath the Kanto-Tokai District, Japan, *J. Geophys. Res.*, **93**, 2076-2094.

JEFFREYS, H., 1939, The times of *P*, *S* and *SKS* and the velocities of *P* and *S*, *Mon. Not. R. Astr. Soc. Geophys. Suppl.*, 4, 498-533.

JORDAN, T. H., 1977, Lithospheric slab penetration into the lower mantle beneath the Sea of Okhotsk, *J. Geophys.*, **43**, 473-496.

KAMIYA, S., T. MIYATAKE and K. HIRAHARA, 1988, How deep can we see the high velocity anomalies beneath the Japan islands?, *Geophys. Res. Lett.*, **15**, 828-831.

MATSUZAWA, T., N. UMINO, A. HASEGAWA and A. TAKAGI, 1986, Upper mantle velocity structure estimated from *PS*-converted wave beneath the north-eastern Japan Arc, *Geophys. J. R. Astr. Soc.*, **86**, 767-787.

MIYAMACHI, H. and T. MORIYA, 1984, Velocity structure beneath the Hidaka Mountains in Hokkaido, Japan, *J. Phys. Earth*, **32**, 13-42.

NAKANISHI, I., 1985, Three-dimensional structure beneath the Hokkaido-Tohoku region as derived from a tomographic inversion of arrival times, *J. Phys. Earth*, **33**, 241–256.

OBARA, K., A. HASEGAWA and A. TAKAGI, 1986, Three dimensional *P* and S wave velocity structure beneath the northeastern Japan arc (in Japanese with English abstract), *Zisin* (*J. Seismol. Soc. Jpn.*), *Ser. 2*, **39**, 201–215.

OKADA, H., S. SUZUKI, T. MORIYA and S. ASANO, 1973, Crustal structure in the profile across the southern part of Hokkaido, Japan, as derived from explosion seismic observations, *J. Phys. Earth*, **21**, 329–354.

OKADA, H., S. ASANO, T. YOSHII, A. IKAMI, S. SUZUKI, T. HASEGAWA, K. YAMAMOTO, K. ITO and K. HAMADA, 1979, Regionality of the upper mantle around northeastern Japan as revealed by big explosions at sea. I. SEIHA-1 explosion experiment, *J. Phys. Earth*, **27**, Suppl., S15–S32.

ROECKER, S. W., H. YEH and Y. B. TSAI, 1987, Three-dimensional *P* and *S* wave velocity structure beneath an arc-continent collision, *J. Geophys. Res.*, **92**, 10547–10570.

SATO, T. and M. KOSUGA, 1987, *P*-wave velocity of the uppermost mantle beneath the source area of the 1983 Japan Sea earthquake (in Japanese with English abstract), *Zisin* (*J. Seismol. Soc. Jpn.*), *Ser. 2*, **40**, 435–444.

SUYEHIRO, K. and I. S. SACKS, 1983, An anomalous low velocity region above the deep earthquakes in the Japan subduction zone, *J. Geophys. Res.*, **88**, 10429–10438.

SUETSUGU, D., 1988, Lower mantle slab penetration as inferred from *P*-wave travel time and amplitude analysis, *Sc. D. thesis, Hokkaido University*.

TAKANAMI, T., 1982, Three-dimensional seismic structure of the crust and upper mantle beneath the orogenic belts in southern Hokkaido, Japan, *J. Phys. Earth*, **30**, 87–104.

WATANABE, I., 1977, The upper mantle structure beneath Japan and its vicinity derived from *P*-wave travel time residuals, *Master thesis, Nagoya University*.

YOSHII, T., 1979, Compilation of geophysical data around the Japanese Islands (I), *Bull. Earthq. Res. Inst., Univ. Tokyo*, **54**, 75–117.

YUHARA, K., 1973, Effect of the Hydrothermal Systems of the Terrestrial Heat Flow, *Bull. Volcanol. Soc. Japan*, **18**, 129–142.

ZHOU, H. and W. CLAYTON, 1988, *P* and *S* wave travel-time inversions for subducting slab under the island arcs of the northwest Pacific, submitted to *J. Geophys. Res.*

日本列島下の3次元P波速度構造

東京大学地震研究所 神谷眞一郎
東京大学地震研究所 宮武隆
京都大学防災研究所 平原和朗

日本列島およびその周辺下 1,200 km までの3次元P波速度構造の詳細なモデルをトモグラフィー手法により得た．データは 833 個の地震による 548 観測点での走時データ 103,032 個 (ISC 報告値)．解を得る際，未知数として震源位置・時刻の要素パラメータと速度構造を同時に求めた．速度構造を求める際に用いたブロックサイズは，水平方向に 0.5°×0.5°，鉛直方向に 50 km (ただし深さ 100 km までは 33 km) である．

その結果，上部マントルの不均質性が詳細に求められた．太平洋プレート，フィリピン海プレートを示す高速度域，火山フロントに対応する低速度域，等々．地殻，マントル上部のほとんどの高速度異常および低速度異常は，それぞれ正・負の重力以上と対応しているが，中国地方のように対応していないところもある．

太平洋プレートの日本海溝からの延長上で地震活動が無くなる深さのさらに先に下部マントルまでのスラブ状の高速度域が得られた．レゾリューション解析から，深さ方向に分解能がないが下部マントルに確かに高速度域が存在することが分かった．一方伊豆—小笠原スラブではこの高速度域は，北緯 26 度付近では 650 km 以深に鉛直方向に分布するが，北緯 29 度付近では 650 km 付近で横たわって見える．